NUEJ
Naresuan University
Engineering Journal

Effect of Weave Pattern on Experimental and Simulated Ballistic Behavior of Carbon Fiber Reinforced Polybenzoxazine Composites.

Kangsadan Inthakun*

Department of Chemical Science and Technology, Chulachomklao Royal Military Academy, Nakhon Nayok, Thailand

*Corresponding author e-mail: Kangsadan.in@crma.ac.th

(Received: 18 April 2024, Revised: 19 June 2024, Accepted: 4 July 2024)

Abstract

This research investigates the effect of weave patterns on the experimental and simulated ballistic performance of carbon fabric reinforced polybenzoxazine (CFR-poly(BA-a)) composites. The present study focuses on developing the materials using a strike panel impacted by a rigid 7.62×51 mm projectile at an impact velocity of 847±9.1. This study compares the ballistic performance of three different weave patterns of CFR-poly(BA-a) composite against the penetration of a 7.62×51 mm projectile by using an energy absorption equation that includes fiber/matrix cohesive failures to predict the appropriate thickness of the composite to protect against penetration. The damage area of the specimen composites is also studied using numerical simulation by using parameters of material properties composite under impact event using 7.62×51 mm projectiles and was performed on 4, 8, and 12 plies of CFR-poly(BA-a) composite. Laminates of three different carbon fabric weave patterns were fabricated using plain, 2x2 twill and unidirectional weaves. The ballistic performance of the composites was investigated by using CFR-poly(BA-a) composite as a strike panel dimensions 150 x 150 mm. The damage area of the specimen composites observed from the experiment results are in good agreement with the numerical simulation model, the error in the prediction of the damage pattern of the specimen composite was less than 3%. The numerical simulation model effectively anticipates the qualitative extent of damage for the composite specimen. The ballistic performance of the composite panel reinforced with a twill weave pattern of carbon fiber observed from the experiment result was superior to that of other weave patterns of carbon fiber due to the 2D woven structure being able to transmit load simultaneously in longitudinal and transverse weave directions. Therefore, it resisted stiffness, stress, and stress distribution. In addition, the twill weave pattern had low contact friction, crimp, and binding effect because of its minimum intersection point compared with plain weave and unidirectional fabrics, therefore relatively high mechanical properties, high energy absorption, and better protection against penetration of the impact velocity of the projectile on the ballistic performance, while also being thinner and lighter when compared with other weaves. These properties make it a more effective material for use in ballistic applications. The numerical simulation and experimental results of the ballistic performance reveal that the hardness of the three weave patterns of CFR-poly(BA-a) composites were able to effectively protect against a single projectile shot without penetration on the rear side of the strike panel, the penetration depth, and damage extent of the perforation were in good agreement with the numerical simulation model. These results suggest the composite could be developed and applied as a strike panel in hard ballistic armor. The findings demonstrate a correlation between numerical simulation outcomes from ballistic impact tests and experimental results, effectively predicting the behavior of CFR-poly(BA-a) composites with relatively low error and good correlation with the experimental data. This predictive capability allows for safe, rapid, and cost-effective design validation and testing by leveraging virtual ballistic impact test models of real-world assets for a person interested in studying them in the future.

Keywords: Composites, Carbon fibers, Woven fabric reinforced polymer (WFRP), Finite element analysis (FEA), Energy absorption.

1. INTRODUCTION

Military confrontations and wars have been a constant throughout world history. As attacking weapons have become more advanced, so too has the level of personal and property protection needed on the battlefield and in riot situations. Different materials have been used as body shields throughout history, from wooden shields to metal shields. Today, ballistic protective materials are primarily used for personnel protection (Al-Haik et al., 2016). These materials are typically lightweight and flexible, making them easy to wear and move in. Ballistic shields are designed as multilayer composite materials that typically consist of hard layers, such as ceramics or steel plates, and soft input materials. When a projectile strikes a hard plate, it can become deformed and cause the fragmentation of the fragile armor, posing a risk to the

user. The function of the soft input layer is to capture and absorb the remaining energy of blunt projectiles and projectile fragments that have damaged the first shielding layer (Pach et al., 2017). In terms of materials used in ballistic armor, steel plates have traditionally been widely used in armor applications in the past. The weight limitation and lack of flexibility of ceramic and steel plates make them less than ideal for use in certain applications, such as body armor (Yashas Gowda et al., 2018; Sherif et al., 2019; Chukov et al., 2019; Linul et al., 2019). Composite materials offer several advantages over traditional materials, such as ceramic and steel, for body armor applications. Composite materials can be designed to be lightweight, have excellent mechanical properties, high thermal properties, outstanding specific modulus, and specific strength (Buehler and Seferi, 2000; Ishida and Chaisuwan, 2003; Li et al., 2013; Delmonte, 1981; Shalin, 1995; Shen and Ishida, 1996). This makes composite materials a good choice for body armor that is both protective and comfortable to wear.

Composite materials are an amalgamation of at least two constituents. Fiber-reinforced polymers (FRPs) are composed of two phases, matrix phase and particle or fiber phase. Fiber textiles are found to be among the most efficient reinforcements for FRPs. Currently, developed fiber-reinforced polymers (FRPs) focus on the relationship between the weave structure property of fibers, different polymer matrices used to develop composites, their mechanical performances, and different composite fabrication techniques (Rajak, 2019). FRP composites are widely used in ballistic protections such as helmets and ballistic armor (Al-Haik et al., 2016; Rebouillat, 2016; Okhawilai and Rimdusit, 2017) due to their excellent mechanical properties including high strength high modulus, and especially extra energy absorption.

Carbon fiber-reinforced polymers (CFRPs) are a class of extremely strong and lightweight fiber reinforced polymers based on carbon/graphite fibers (Che et al., 2014). CFRPs offer a very high strength-to-weight ratio, high modulus-to-weight ratio (specific modulus), high damping capacity, good dimensional stability, excellent damage tolerance, and good corrosion and fatigue resistances, which makes them widely used in aerospace, robotics (Wang et al., 2003), construction, transportation, sporting goods, medical, and military applications (Dandekar et al., 2012).

The knitting pattern can affect the mechanical properties of a textile, which in turn affects the composite mechanical properties (Ratna et al., 2004; Hallal et al.,2012; Colorado et al., 2006). By carefully selecting the knitting pattern, it is possible to design FRPs with the desired mechanical properties. Woven fabric-reinforced polymer (WFRP) composites have excellent mechanical strengths, i.e., rigidity, strength, and dimensional stability compared to unidirectional fiber composites. WFRPs are particularly attractive for lightweight structures because of their high strength-to-weight ratios, directional tolerability, and strength dependencies on strain rates. These highly engineered materials are increasingly sought after for use in structures and protective devices required to operate and survive against severe dynamic loading events such as blast, ballistic and fragment impacts, and mechanical shock. Textile engineering concepts can be used to improve the mechanical properties of hybrid woven composites. This can be achieved by selecting the appropriate yarn size, as the correct choice of yarn size can provide the optimal force value and strength to resist the deformation of the woven fabric and ensure the good mechanical properties of the composites (Wahab, 2014).

The following are some research areas related to the use of textile engineering concepts to enhance the mechanical properties of hybrid woven composites Cavallaro (2016) investigated the effects of weave styles and crimp gradients (CGs) on the damage tolerance levels and energy absorption capacities of woven fabric reinforced polymer (WFRP) composites. A comparative study was conducted to determine the specific failure mechanisms including fiber/matrix cohesive failures, matrix cracking, fiber breakage, and fiber buckling resulting from static and dynamic loading events. The tests included flexure, short beam shear, drop impact, flexure-after-impact, ballistic impact, and split Hopkinson compression bar (SHCB) and were performed on 20-ply Kevlar/epoxy WFRP laminates. Laminates of three different Kevlar fabric weave styles were fabricated using plain, 2×2 twill, and 4H satin weaves. A fourth laminate was constructed having a mixture of weave styles forming a hybrid crimp gradient construction. The experimental results demonstrated that weave style selection and CGs can positively influence the spatial and temporal distributions of stress resulting from severe loading events and (that the fiber/ matrix cohesive zone stresses that often lead to delamination can be reduced. Accordingly, the dependence of mechanical performance on weave styles, crimp contents, and CGs can be exploited to increase the damage tolerance levels and energy absorption capacities in WFRP composites.

Ullah and Harland (2014) performed dynamic flexure testing of 4-ply woven-glass and woven-carbon laminates using a pendulum fixture. Both laminates were constructed of twill (2×2) fabric architectures and thermoplastic polyurethane (TPU) matrices. Computer tomography (CT) scans were used to examine the damage zones, which revealed that the damage mechanisms consisted of matrix cracking, delamination, yarn debonding, and fiber breakage. Numerical The Finite Element Method (FEM) was performed using cohesive zone elements, quadratic stress criterion for damage initiation, and the Benzeggagh-Kenane criterion for damage evolution. The carbon-fiber-reinforced polymer (CFRP) laminates exhibited lower fracture toughness and higher impact strengths than the glass-fiber-reinforced polymer (GFRP) laminates. The FEM results correlated

to the test results and captured the sequence of failure modes.

Research by Cavallaro and Sadegh (2010) was performed on single-ply woven fabrics subjected to ballistic impact using ABAQUS/Explicit analysis. Their numerical modeling results demonstrated that, compared to crimp-balanced woven fabrics, crimp-imbalanced woven fabrics can achieve greater dynamic energy absorption capacities for normal and oblique impacts. They further showed that crimp imbalance can minimize stress-wave reflections at the crossover region and can positively alter the spatial and temporal behaviors of stress wave propagations within the fabrics.

Another important factor influencing FRP composites' ballistic performance is the polymer matrix type because it is the binder that combines all of the reinforcement. Polybenzoxazines are a novel class of phenolic resin that undergoes polymerization via the ring-opening reaction of cyclic benzoxazine resins under thermal conditions. This process obviates the requirement for a catalyst or curing agent and does not generate any by-products during thermal polymerization (Chung, 2017; Ratna et al., 2004; Hallal et al.,2012; Haim, 2017). Polybenzoxazines exhibit superior characteristics upon polymerization including dimensional stability, near-zero volumetric shrinkage, and low water absorption (Cavallaro et al., 2006). The polymerization reaction of benzoxazine resins also generates phenolic moieties which are highly useful functional groups that facilitate further interaction with other fibers or fillers and enable further modification with other chemicals, resins, or polymers in the network formation of polybenzoxazine (Dipen, 2019; Wahab, 2014). This versatility allows for the tailoring of properties to meet the requirements of numerous applications, including ballistic protection. Gopinath et al., (2012) suggested that the interaction between the polymer matrix and reinforcement was one of the most important factors affecting impact response. They found that the deformation area was decreased with the presence of the appropriated interactions between the stiff matrix and yarns because their excessive interaction and embedded yarns would restrict the movement of yarns, thereby reducing energy absorption and the ballistic performance of the composites.

Okhawilai et al., (2018) investigated the impact performance of the strike panel composite based on glass fiber reinforced polybenzoxazine composites. Experimental panels were manufactured from E-glass and S-glass fiber reinforced polybenzoxazine backed by aramid fiber reinforced composites and subjected to 7.62 × 51 mm rifle projectile at a high velocity of 847 ± 9.1 m/s. Based on the test results, the specimens were able to protect against perforation by the projectile. Comparing the same number of plies, cone deformation on the last panel of S-glass composite was significantly lower than that of the specimen manufactured using E-glass composite. Less damaged area and depth of penetration on backing panels of S-glass composites were significantly observed when compared to that of E-glass specimens under the ballistic test. The authors that the high tensile modulus of the strike panel could result in superior ballistic impact response in terms of both reduction in back face deformation and depth of penetration on the back side of the backing panel. Moreover, the hardness of the strike panel indicated an ability to destroy the projectile into fragments with no failure on the backing panel. This result also revealed a potential use of S-glass fiber reinforced polybenzoxazine composite as a strike panel for hard ballistic armor. Therefore, the important properties i.e. appropriated interaction between matrix-fiber, hardness, and tensile modulus of the strike panel materials are key parameters for reducing back face deformation and depth of penetration on the back side of the backing panel. The authors that the interaction between the polymer matrix and reinforcement was one of the most important factors affecting the impact response. They found that the deformation area was decreased with the presence of the appropriated interactions between the stiff matrix and yarns because their excessive interaction and embedded yarns would restrict the movement of yarns to dissipate the energy absorption and ballistic performance of the composites decreased.

Furthermore, the important issue encountered in the study of penetration mechanics under ballistic impact is the determination of ballistic limit velocity, which refers to a critical velocity below which a projectile could perforate the armor. Many attempts have studied the effect of impact velocity and residual velocity of the projectile on the ballistic limit velocity for a variety of materials (Chocron et al., 2010; Flores-Johnson et al., 2014; Ansari and Chakrabarti, 2017; Sevkat et al., 2009). Due to the complex ballistic penetration process, numerical simulation is used to predict the ballistic performance and study ballistic behavior.

Ansari and Chakrabarti (2017) have studied the experimental and finite element analyses of perforation behavior of unidirectional glass fiber reinforced cross-ply laminate, by considering different projectile nose shapes, impact velocities, impact angles, and laminate thickness. A three-dimensional finite element model was developed using Lagrangian, eight nodded brick elements in ANSYS/AUTODYN. The properties of GFRP laminate were obtained from tensile tests in a Universal Testing Machine. The ballistic limit and damage pattern in the target plate are presented and compared. They revealed that the obtained results from numerical simulation had a good correlation with the corresponding experimental values.

Sevkat et al., (2009) studied the damage in composite beams subject to ballistic impact using a high-speed gas gun by a combination of experimental and 3D dynamic nonlinear finite element (FE) analysis. LS-DYNA with the Chang–Chang linear-orthotropic damage model was used for comparison. They found good agreement between experimental and FE results from the

comparisons of damage patterns. Moreover, FE simulations were conducted to predict the ballistic limit velocity (V_{50}) using either the number of damaged layer approach similar to the classical Lambert–Jonas equation for metals.

Naik et al., (2000) performed 3-D FEM modeling of thin woven and UD cross-ply E-glass/epoxy laminated plates subjected to low-velocity impact. An in-plane failure function based on the Tsai-Hill criterion was used to assess damage initiation during impact (failures occurred when the failure function achieved a magnitude≥1.0). Their results demonstrated that the in-plane failure function magnitudes were greater along the impact surfaces versus the rear surfaces of the woven laminates suggesting that in-plane failures would initiate near the impact surfaces, and greater along the rear surfaces of the UD cross-ply laminate suggesting that in-plane failures would initiate near the rear surfaces. However, the failure function magnitudes reported for the cross-ply laminates were approximately five times greater than those of the woven laminates. Based upon the in-plane failure criterion alone, the woven laminates achieved a five times greater damage initiation threshold for low-velocity impact than that for the UD cross-ply laminates.

Therefore, in this work, a comparative study of the ballistic performance of three different weave patterns of (CFR-poly(BA-a)) composite against the penetration of a 7.62×51 mm projectile by using an energy absorption equation that includes fiber/matrix cohesive failures to predict the appropriate thickness of the composite to protect against penetration. The damage area of the specimen composites is also studied by comparing the experimental and numerical simulations and predicting the penetration depth and damage extent of the perforation observed in the strike panel by numerical simulation. The focus of the present study is to develop CFR-poly(BA-a) composite for use as strike panels that can be impacted by a rigid 7.62×51 mm projectile at an impact velocity of 847±9.1 m/s. It was investigated using numerical simulation to predict the behavior of composites. The predictive capability allows for safe, rapid, and cost-effective design validation and testing by leveraging virtual ballistic impact test models of real-world assets for a person interested in studying them in the future.

2. MATERIALS AND PREPARATION

2.1 Materials

The composite materials studied in this research were manufactured using benzoxazine resin (BA-a) based on bisphenol-A, formaldehyde, and aniline as the polymer matrix reinforced with textiles made of carbon. The bisphenol-A (polycarbonate grade) was kindly supplied by Thai Polycarbonate Co., Ltd. (Rayong, Thailand). Formaldehyde (AR grade) and aniline (AR grade) were purchased from Merck Co., Ltd. and Panreac Quimica, S.A., respectively. Three weave styles were sourced: plain, twill, and unidirectional carbon fabric weaves with area weight densities of 1.507, 1.507, and 1.526 g/cm^3, respectively. These fabrics were used as reinforcing fabrics and were purchased from BRP Composite Limited Partnership (Thailand). All chemicals and the carbon fiber were used as received.

2.2 Resin preparation

BA-a resin was synthesized from bisphenol A, formaldehyde, and aniline at a molar ratio of 1:4:2 based on solvent-less technology (Ishida, 1996). The mixture solution was continuously stirred at 110°C for approximately 40 min. The obtained resin was in a clear homogenous mixture with a yellowish color and solid at room temperature. The solid resin was ground into fine powder and kept in a refrigerator before copolymer preparation.

2.3 Sample preparation

The samples in this study consist of composite panels, also known as strike panels. The strike panels were prepared from 65%wt of CFR-poly(BA-a) composite (Inthakun, 2023). The plain, twill, and unidirectional weave patterns of carbon fabric with approximate dimensions of 150 mm x 150 mm consisting of 4, 8, and 12 plies of carbon fiber were coated with the BA-a resin using a hand lay-up procedure. This procedure was employed to fabricate the laminated composite panels at 120°C to yield the prepregs. The obtained prepregs were stacked and preheated at 180°C for 20 minutes, 200°C for 10 minutes, and fully cured at 200°C for 2 hours in a compression molder using a pressure of 15 MPa. All samples were air-cooled to room temperature in the open mold. The plain, twill, and unidirectional weave patterns of CFR-poly(BA-a) composites consist of 4, 8, and 12 plies as shown in Figure 1.

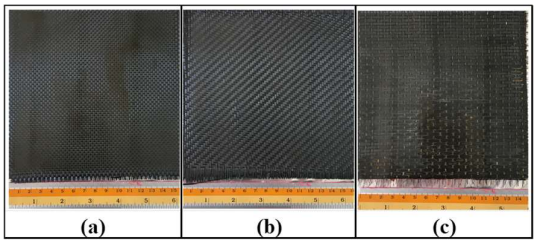

Figure 1 The weave patterns of CFR-poly(BA-a) composites (a) The plain, (b) twill, and (c) unidirectional

2.4 Characterization

2.4.1 Ballistic performance of the samples

The ballistic impact test was performed at the shooting range of Chulachomklao Royal Military Academy, Nakhon Nayok, Thailand. The tests were conducted using cartridges to propel projectiles onto composite specimens which were laminated from three weave patterns of CFR-poly(BA-a) composite containing carbon fiber at 4, 8, and 12 plies. On the impact test of the

projectiles, two sets of chronograph units were placed at 2 m in front and behind the target acquisition unit to record the impact and residual velocities of the projectiles, respectively. The 150×150 mm^2 composite plate was clamped in the target holder and placed on a steel frame at 15 m in line with the gun barrel and subjected to the impact of the projectiles. The tests were conducted using a high-level ballistic impact test based on NIJ standard level III using 7.62×51 mm projectiles at an impact velocity of 847±9.1 m/s at an angle of 90° to the specimen for one shot at the center. The initial impact velocity was measured by placing optical sensors in the field which were connected to a data acquisition system. The 7.62×51 mm projectiles have a diameter of 7.79 mm and a mass of 9.65 g as shown in Figure 2. The experimental setup is shown in Figure 3. The energy absorption of the composite specimen was determined by the difference between the initial kinetic energy and the final kinetic energy according to Equation (1).

$$E_a = 1/2m_p(V_s^2-V_r^2) \quad (1)$$

where E_a is energy absorption of the sample (J), m_p is the mass of a projectile (kg), V_s is impact projectile velocity (m/s) and V_r is residual projectile velocity after penetrating through the sample (m/s), respectively. This equation is under the assumption of the undeformed projectile.

Figure 2 7.62x51 mm FMJ NATO projectiles used.

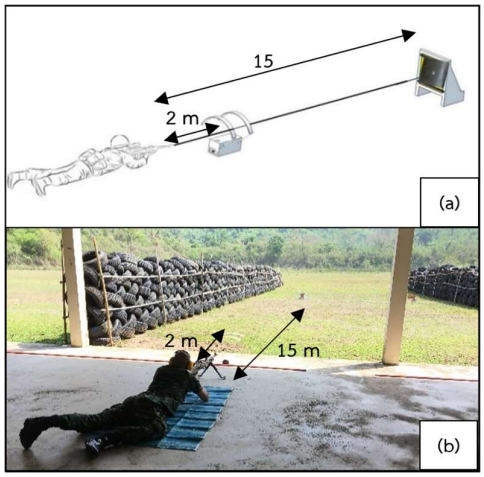

Figure 3 The experimental setup for high-velocity ballistic impact tests. (a) the schematic of the experimental setup and (b) the actual experimental setup.

2.4.2 Morphology of the samples

Sample morphology was studied using a scanning electron microscope (SEM, model JSM-IT300 from JEOL Ltd. (Tokyo, Japan)) using an acceleration voltage of 15 kV. All samples were coated with a thin layer of gold film using a sputter coater to make the surfaces conductive.

2.4.3 Numerical Simulations of ballistic characteristics

Numerical simulations of the experimental ballistics tests were conducted using finite element analysis (FEA) is the process of predicting an object's behavior based on calculations made with the finite element method (FEM). While FEM is a mathematical technique, FEA is the interpretation of the results FEM provides. FEA is insights into complex systems and structures, helping make more informed design decisions. FEA is the application of FEM equations and is the basis of many types of simulation software. It's used to validate and test designs safely, quickly, and economically by creating virtual models of real-world assets (Ferris, 2024).

The numerical modeling approach previously described was used to simulate all configurations of the ballistic impact carried out in the experimental tests. Moreover, the same approach was subsequently used as a virtual test environment to enrich (virtually) the data by obtaining the full ballistic curve for each configuration, allowing the determination of the ballistic limit by best fitting the impact data to the Recht-Ipson curve (Recht and Ipson, 1963) using the nonlinear least square method.

2.4.3.1 Comparison of the experimental and numerical method

The ballistic performance and the damage pattern of twill weave patterns of CFR-poly(BA-a) composite at the thickness of 1, 1.85, and 2.70 mm., respectively were studied using a series of numerical simulations. The impact test on specimens with dimensions of 150 × 150 mm^2 was tested using 7.62 × 51 mm projectiles at various impact velocities. The perforation process and deformation of the specimen were evaluated numerically with a commercial ANSYS AUTODYN system by using the material properties of the composite in parameters of young modulus, Poisson's ratio, strength: shear modulus, failure: tensile failure stress or strain, failure: tensile failure strain, density, and thickness, presented in Table 1 from Inthakun (2023) for the simulation evolution of the projectile penetrating process of composite panels. Then measure the extent of the experimental damage area composite and damaged area predicted from the numerical analysis on both the front and rear view of the specimen. Finally, calculate the percentage of the difference between the experimental and predicted damage area according to Equation (2).

$$\frac{(w_p-w_{exp})\,x\,(l_p-l_{exp})}{A_{d(exp)}} \text{ x } 100 \quad (2)$$

where w_p is the width of the predicted damage area (mm), w_{exp} is the width of the experimental damage area composite (mm), l_p is the length of the predicted damage area (mm), l_{exp} is the length of the experimental damage area composite (mm), $A_{d(exp)}$ is the damage area of the experimental (mm^2), respectively.

2.4.3.2 The ballistic performance predicted the thickness confirmed by numerical simulation

Numerical simulation analysis was used to evaluate the ballistic impact behavior of hard armor prepared from strike panel based on poly(BA-a) composite prepared from the plain, twill, and unidirectional weave of CFR-poly(BA-a) composites at thicknesses of 48.7, 45.2, and 65.7 mm, respectively. The 150 × 150 mm^2 specimens were tested by 7.62 × 51 mm projectiles at an impact velocity in the range of 847±9.1 m/s for one shot. Ballistic testing of the specimen was evaluated numerically with a commercial ANSYS AUTODYN system using the material properties of the composite presented in Table 2 from (Inthakun, 2023) for the simulation evolution of the projectile penetrating process of composite panels.

Table 1 Material properties of twill weave CFR-poly(BA-a) by various thickness (Inthakun, 2023).

Properties		Twill weave pattern of CFR-poly(BA-a) composite		
		4 plies	8 plies	12 plies
Thickness, mm		1.00	1.85	2.70
Density, g/cm³		1.46		
Young modulus, kPa	E_{11}	3.83×10^7		
	E_{22}	3.83×10^7		
	E_{33}	2.60×10^6		
Poisson's ratio	ν_{12}	0.07		
	ν_{23}	0.7		
	ν_{31}	0.075		
Strength: Shear modulus, kPa	G_{12}	5.8×10^5		
	G_{23}	1.7×10^4		
	G_{31}	1.7×10^4		
Failure: Tensile failure stress or strain	σ_{11}	8.3×10^5		
	σ_{22}	7.2×10^5		
	σ_{33}	7×10^4		
Failure: Tensile failure strain	ε_{11}	0.012		
	ε_{22}	0.014		
	ε_{33}	0.02		

Table 2 Material properties of each weave pattern composite panels (Inthakun, 2023).

Properties		Weave patterns of CFR-poly(BA-a) composite		
		Plain	Twill	UD
Thickness, mm		48.7	45.2	65.7
Density, g/cm³		1.43	1.46	1.45
Young modulus, kPa	E_{11}	3.64×10^7	3.83×10^7	3.58×10^7
	E_{22}	3.64×10^7	3.83×10^7	3.58×10^7
	E_{33}	2.48×10^6	2.60×10^6	2.43×10^6
Poisson's ratio	ν_{12}	0.07	0.07	0.07
	ν_{23}	0.7	0.7	0.7
	ν_{31}	0.075	0.075	0.075
Strength: Shear modulus, kPa	G_{12}	5.5×10^5	5.8×10^5	4.8×10^5
	G_{23}	1.7×10^4	1.7×10^4	1.7×10^4
	G_{31}	1.7×10^4	1.7×10^4	1.7×10^4
Failure: Tensile failure stress or strain	σ_{11}	7.2×10^5	8.3×10^5	10.3×10^5
	σ_{22}	7.2×10^5	7.2×10^5	1.7×10^5
	σ_{33}	7×10^4	7×10^4	7×10^4
Failure: Tensile failure strain	ε_{11}	0.013	0.012	0.018
	ε_{22}	0.013	0.014	0.11
	ε_{33}	0.02	0.02	0.02

3. RESULTS AND DISCUSSION

3.1 Effect of thickness on the ballistic performance of CFR-poly(BA-a) composite

The relationship between energy absorption and thickness of three different CFR-poly(BA-a) composite weave patterns. The fabric weaves included the plain pattern interlaced one up and down, the 2x2 twill interlaced two up and down, and unidirectional patterns in all the fibers running in a single, parallel direction. Specimens with various thicknesses as thin as the projectile were tested under impact event using 7.62×51 mm projectiles at an average velocity (V_s) of 847 ± 9.1 m/s according to NIJ at level III. Energy absorption was calculated using Equation (1) and plotted in Figures 4-6. The results demonstrated that the energy absorption value of the composite during the ballistic impact test increased with increasing thickness for all three weave pattern specimens composite. The results indicated an effective stress transfer between plies with thicker composites

because thicker composite layers produce heavier and increased fiber composite areal density to enhance the impact performance under high impact velocity (Colakoglu et al., 2007). Evaluation of the energy absorption E_a values with specimen thickness revealed a relatively nonlinear increase with increasing thickness of the composite. Quadratic fit gives exponents depicting the dependence of E_a of the plain, twill, and unidirectional weave of CFR-poly(BA-a) composite with the exponent values of 0.1277, 0.1451, and 0.0563, respectively (Carrillo J.G. et al, 2012).

The experimental results showed that the highest energy absorption was from the specimen reinforced with a twill weave pattern of CFR-poly(BA-a) composite presented in Figure 7, its high flexural strength and impact resistance properties due to the 2D woven structure were able to transmit load simultaneously in longitudinal and transverse weave directions. Therefore, it resisted stiffness, stress, and stress distribution. As in the weave structure of composite, it could be seen that twill weave had low contact friction, crimp, and binding effect because of its minimum intersection point compared with plain weave and unidirectional fabrics, therefore twill weave is a low level of fiber crimp impart relatively high mechanical properties compared with other weaves (Tong L. et al., 2002; Cavallaro, 2016). The damage figure in the front and rear view of CFR-poly(BA-a) composite specimen after impact with 7.62×51 mm projectiles is shown in Figure 8. The results demonstrated that the estimated residual kinetic energy of the projectile was significantly decreased with increasing thickness of the specimen composite. The estimated residual kinetic energy of the projectile was reduced to lower or equal to zero, exhibiting full ballistic protection from those projectiles.

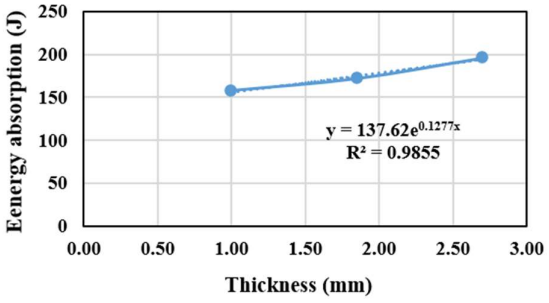

Figure 4 Relationship between energy absorption and thickness of plain weave CFR-poly(BA-a) composite.

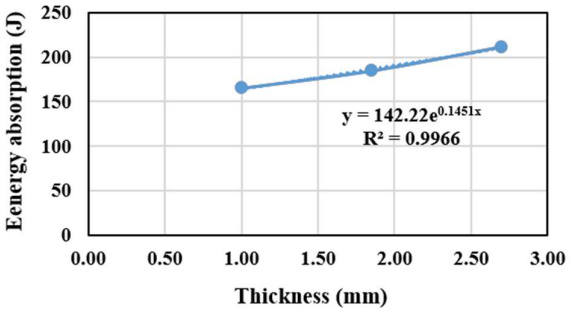

Figure 5 Relationship between energy absorption and thickness of twill weave CFR-poly(BA-a) composite.

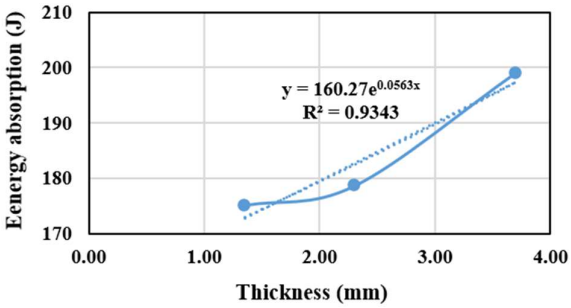

Figure 6 Relationship between energy absorption and thickness of unidirectional weave CFR-poly(BA-a) composite.

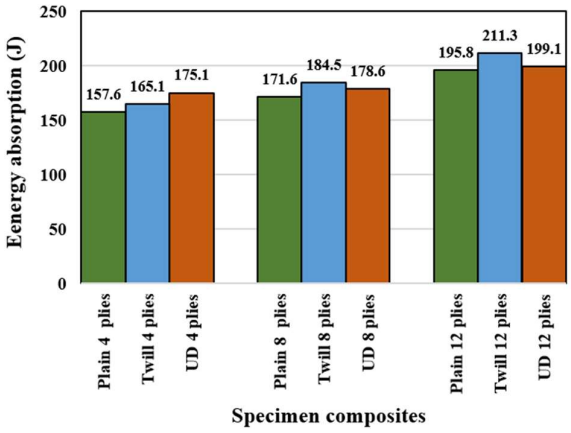

Figure 7 Relationship between energy absorption and the pile of each specimen composite

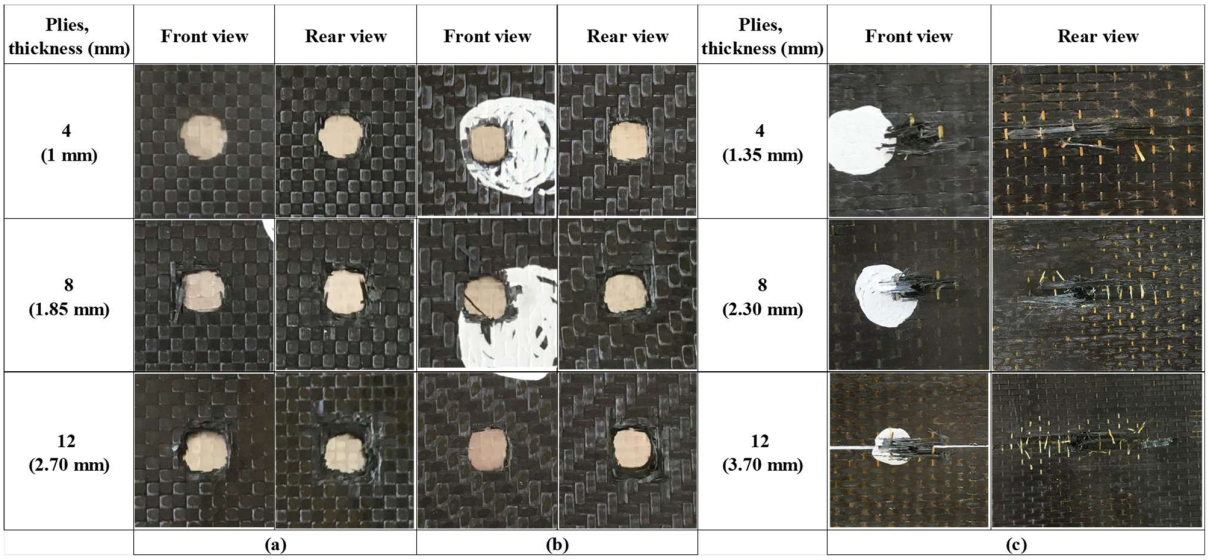

Figure 8 The damage figure in front and rear view of CFR-poly(BA-a) composite
(a) The plain, (b) twill, and (c) unidirectional weave pattern after impact with 7.62×51 mm projectiles

The results suggested that the suitable thickness tested by 7.62×51 mm projectile at an upper impact velocity of the plain, twill, and unidirectional weave of CFR-poly(BA-a) composite was 48.7, 45.2, and 65.7 mm, respectively, and the estimated energy absorption of specimen composites was found to be as high as 3536.28 J as shown in Table 3. The estimated residual kinetic energy was calculated using the nonlinear ballistic equation and Equation (1). However, to produce armor or strike panels for ballistic protection of projectiles of CFR-poly(BA-a) composite, the twill weave pattern of CFR-poly(BA-a) composite was stronger than any other weave pattern of CFR-poly(BA-a) composite because the twill weave pattern of CFR-poly(BA-a) composite has the highest energy absorption and the thinnest thickness for supporting the upper impact velocity of ballistic when compared with other weave patterns of CFR-poly(BA-a) composite.

Table 3 The thickness and energy absorption of three weave patterns of CFR-poly(BA-a) composite

Weave of specimen composite	Calculation of the specimen composite*	
	Thickness (mm)	Energy absorption (J)
Plain	48.7	3536.28
Twill	45.2	
UD	65.7	

* Calculation by use of 7.62×51 mm projectiles at an impact velocity of 847±9.1 m/s

3.2 Morphological Analysis

The fracture surface of CFR-poly(BA-a) composite after impact with 7.62×51 mm projectiles is also studied by Scanning electron microscopy (SEM) micrographs at 1500x magnification were taken of the warp region of the plain, twill, and unidirectional weave patterns of CFR-poly(BA-a) composite, as shown in Figure 9 (a), Figure 9 (b), and Figure 9 (c), respectively.

The SEM micrographs indicate that the carbon fabric of the plain and twill weave patterns was potentially adhered to the poly(BA-a) matrix, as can be observed from the pieces of matrix attached to the fiber, similar to the specimen composite before impact testing with 7.62×51 mm projectiles, as shown in Figure 9 (a) and Figure 9 (b). The CFR-poly(BA-a) composite of unidirectional weave pattern in the warp region shows adhesive and cohesive fracture due to matrix debonding, fibers pulled out, and breakage fibers when compared with the specimen composite before impact testing with 7.62×51 mm projectiles, as shown in Figure 9 (c). Moreover, the fracture surface is extensively embedded with poly(BA-a) matrix to correspond with the damage photo of CFR-poly(BA-a) composite specimen as shown in Figure 8. This implies that cohesive failure occurred in the poly(BA-a) matrix region due to the significant improvement in the interfacial adhesion between the carbon fabric and the poly(BA-a) matrix (Taraghi, 2014).

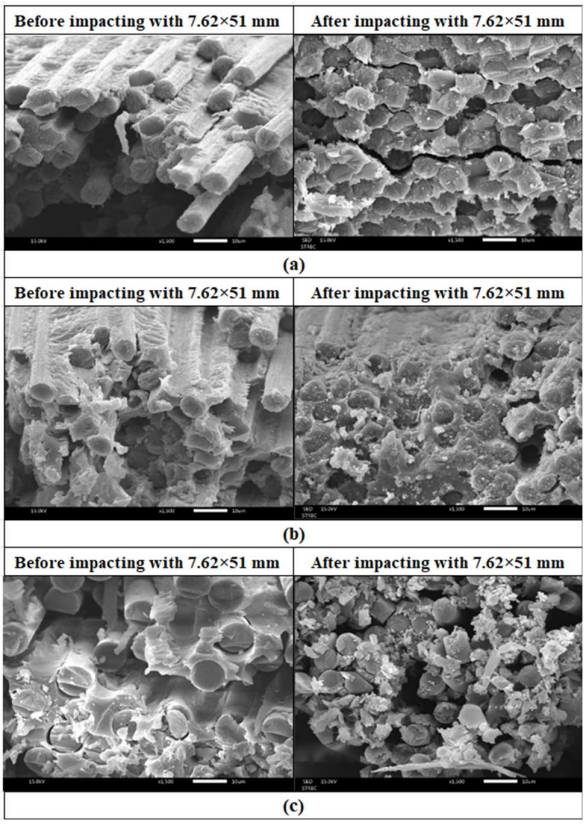

Figure 9 The scanning electron microscope at 1500x of CFR-poly(BA-a) composite in warp region filled before and after impacting with 7.62×51 mm (a) The plain weave pattern, (b) The twill weave pattern (c) The unidirectional weave pattern

3.3 Comparison of the experimental and numerical results

The experimental and numerical results of ballistic impact tests in terms of the damage areas on both the front and rear sides of the composite specimen at various thicknesses, as shown in Figures 10-12. The numerical simulation model qualitatively predicted the extent of damage for the specimen. From Figure 10, the extent of the experimental damage area of the composite was measured to be 8 mm × 7 mm, while the predicted damage extent measured 9 mm × 8 mm. The difference between the experimental and predicted damage area was approximately 2%.

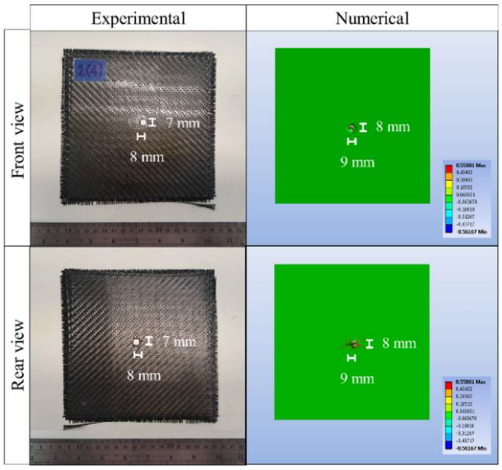

Figure 10 Comparison of the experimental and numerical damage areas of the poly(BA-a) composite at the thickness of 1 mm.

Figure 11, the extent of the experimental damage area of the composite was measured to be 9 mm × 7 mm, while the predicted damage extent measured 11 mm × 8 mm. The difference between the experimental and predicted damage area was approximately 3%.

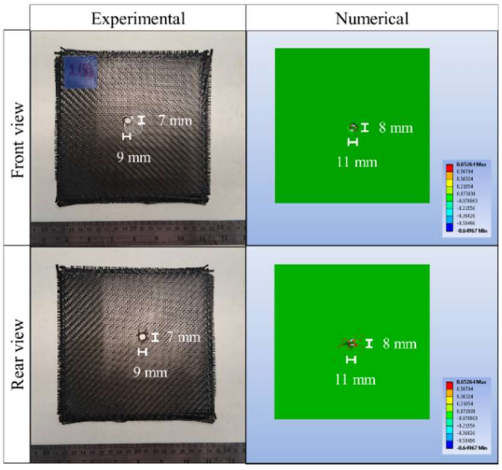

Figure 11 Comparison of the experimental and numerical damage areas of the poly(BA-a) composite at the thickness of 1.85 mm.

Figure 12, the extent of the experimental damage area of the composite was measured to be 10 mm × 10 mm, while the predicted damage extent measured 12 mm × 11 mm. The difference between the experimental and predicted damage area was approximately 2%.

From the results, the experimental results are in good agreement with the numerical simulation model. The numerical simulation model also did a good job of qualitatively predicting the extent of the damage for this specimen (Ansari and Chakrabarti, 2017).

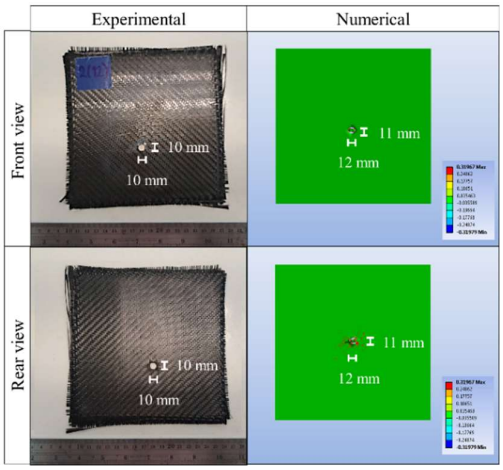

Figure 12 Comparison of the experimental and numerical damage areas of the poly(BA-a) composite at the thickness of 2.70 mm.

3.4 The ballistic performance predicted the thickness confirmed by the numerical simulation result

The results revealed that the plain, twill, and unidirectional weave pattern of CFR-poly(BA-a) composites could protect against projectiles one shot without perforation on the back side of the strike panel. The penetration depth and damage extent of the perforation observed in the strike panel in the side and rare view were in good agreement with the numerical simulation model shown in Figure 11. The result indicated a strike panel for hard armor based on polybenzoxazine composites which was prepared from a strike panel of plain, twill, and UD weave patterns of CRF-poly(BA-a) composite with thicknesses was 48.7, 45.2, and 65.7 mm, respectively, could completely protect against projectiles one shot without the perforation on the rear side of the strike panel tested by 7.62 × 51 mm projectiles at an impact velocity in the range of 847±9.1 m/s.

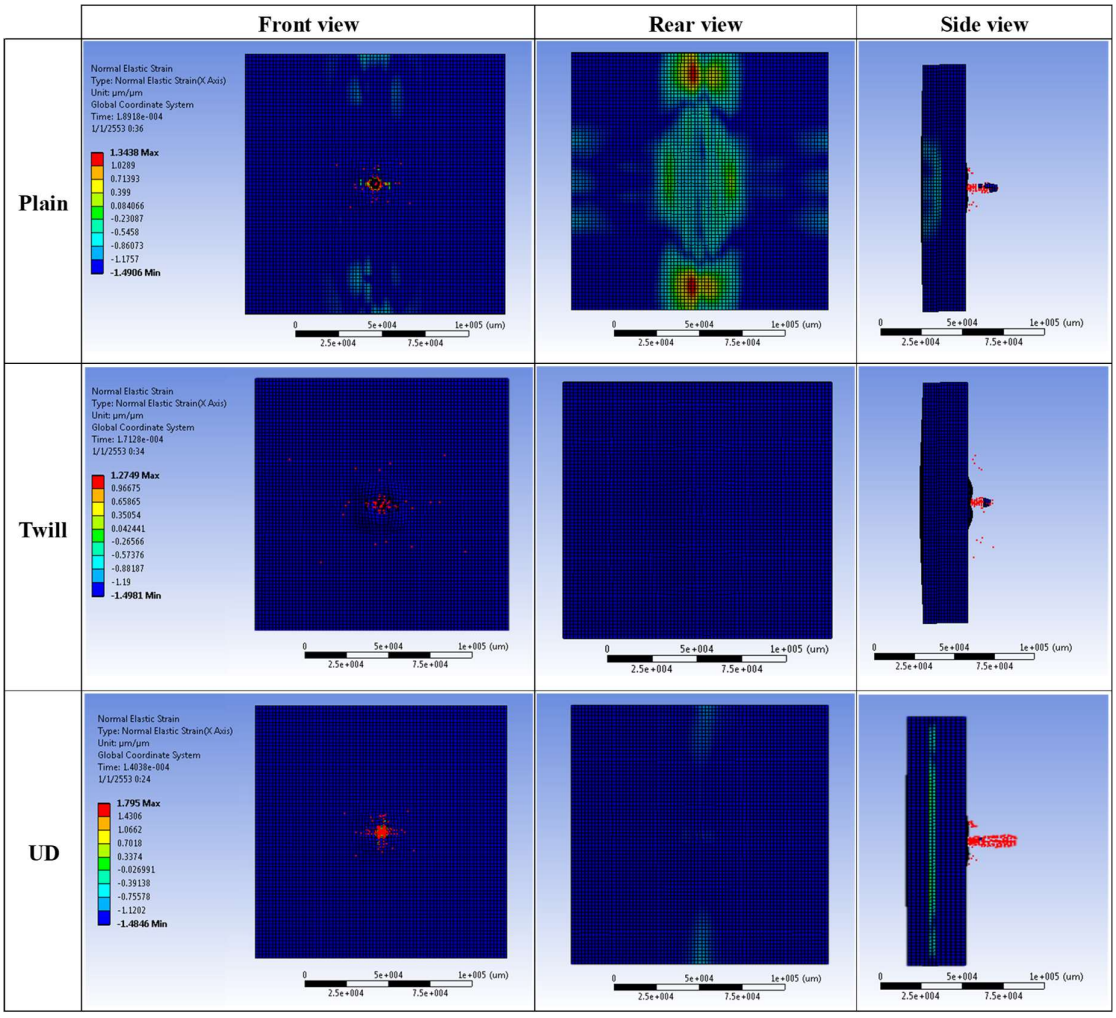

Figure 11 One-shot performance by numerical simulation of a strike panel based on three weave patterns of CFR-poly(BA-a) composite.

4. CONCLUSION

The numerical simulation results obtained were compared with experimental data to verify the suitable thickness for the ballistic protection of 7.62×51 mm projectiles. A satisfactory correlation of the suitable thickness of three weave patterns of CFR-poly(BA-a) composite was achieved with experimental observations. In particular, the error in the prediction of the difference between the experimental and predicted damage area was less than 3%. Moreover, the suitable thickness of the developed composites was predictable using the obtained energy absorption equation. Furthermore, the specimen based on CFR-poly(BA-a) composites at the appropriate thickness can protect against the penetration of 7.62×51 mm projectile at a velocity of 847±9.1 m/s. The results demonstrated that the energy absorption value of the composite during the ballistic impact test increased with increasing thickness for all three weave pattern composites. The results indicated an effective stress transfer between plies with thicker composites because thicker composite layers produce heavier specimens and initiate increased areal density of fiber composite to enhance the impact performance under high impact velocity. The predicted thickness of plain, twill, and unidirectional weave pattern CFR-poly(BA-a) composite was found to be 48.7, 45.2, and 65.7 mm, respectively. The result of the energy absorption of the twill weave pattern CFR-poly(BA-a) composites was the highest because the 2D woven structure could transmit load simultaneously in longitudinal and transverse weave directions. Therefore, it resisted stiffness, stress, and stress distribution. As in the weave structure of composite, it could be seen that twill weave had low contact friction, crimp, and binding effect because of its minimum intersection point compared with plain weave and unidirectional fabrics, therefore twill weave is a low level of fiber crimp impart relatively high mechanical properties compared with other weaves to corresponding with morphological analysis. Moreover, the hardness of three weave pattern CFR-poly(BA-a) composites from experimental conformed to the ballistic performance result by numerical simulation could protect against projectiles one shot without the perforation on the rear side of the strike panel. Results revealed that the CFR-poly(BA-a) composites have high ballistic performance to be utilized as a strike panel for hard armor applications. The findings demonstrate a correlation between numerical simulation outcomes from ballistic impact tests and experimental results, effectively predicting the behavior of CFR-poly(BA-a) composites with relatively low error and good correlation with the experimental data. This predictive capability allows for safe, rapid, and cost-effective design validation and testing by leveraging virtual ballistic impact test models of real-world assets for a person interested in studying them in the future.

5. ACKNOWLEDGMENT

This work was supported by the Chulachomklao Royal Military Academy Development Fund in the year 2019 from Chulachomklao Royal Military Academy. The authors gratefully acknowledge Prof. Sarawut Rimdusit, Ph.D., and Dr. Phattarin Mora for their consulting advice in conducting the research.

6. REFERENCES

Al-Haik, M., Borujeni., A. Y., & Tehrani, M. (2016). 5-Ballistic damage of hybrid composite materials. *In Advanced Fibrous Composite Materials for Ballistic Protection*, 121-143. https://doi.org/10.1016/B978-1-78242-461-1.00005-4

Pach, J., Pyka, D., Jamroziak, K., & Mayer, P. (2017). The experimental and numerical analysis of the ballistic resistance of polymer composites. *Composite. Part B Engineering, 113*, 24-30. https://doi.org/10.1016/ j.compositesb.2017.01.006

Yashas Gowda, T.G., Sanjay, M.R., Subrahmanya Bhat, K., Madhu, P., Senthamaraikannan, P., & Yogesha, B. (2018). Polymer matrix-natural fiber composites: An overview. *In Cogent Engineering, 5(1)*, 1-13. https://doi.org/10.1080/23311916.2018.1446667

Sherif, G., Chukov D., Tcherdyntsev V., & Torokhov V. (2019). Effect of Formation Route on the Mechanical Properties of the Polyethersulfone Composites Reinforced with Glass Fibers. *Polymers, 11(8)*, 1364. https://doi.org/10.3390/polym11081364

Chukov, I. D., Nematulloev, S., Zadorozhnyy, M., Tcherdyntsev, V., Stepashkin, A., & Zherebtsov, D. (2019). Structure, mechanical and thermal properties of polyphenylene sulfide and polysulfone impregnated carbon fiber composites. *Polymers, 11(4)*, 684. https://doi.org/10.3390/polym11040684

Linul, E., Lell, D., Movahedi, N., Codrean, C., & Fiedler, T. (2019). Compressive properties of zinc syntactic foams at elevated temperatures. *Composites Part B: Engineering, 167*, 122-134. https://doi.org/10.1016/ j.compositesb.2018.12.019

Buehler, F.U., & Seferis, J.C. (2000). Effect of reinforcement and solvent content on moisture absorption in epoxy composite materials. *Composites Part A: Applied Science and Manufacturing, 31(7),* 741-748. https://doi.org/ 10.1016/S1359-835X(00)00036-1

Ishida, H., & Chaisuwan, T. (2003). Mechanical property improvement of carbon fiber reinforced polybenzoxazine by rubber interlayer, *Polymer Composites, 24(5)*, 597-607. https://doi.org/10.1002/ pc.10056

Li, W., Yao, S.Y., Ma, K.M., & Chen, P. (2013). Effect of plasma modification on the mechanical properties of carbon fiber/phenolphthalein polyaryletherketone composites. *Polymer Composites, 34(3)*, 368-375. https://doi.org/10.1002/pc.22385

Delmonte, J. (1981). *Technology of Carbon and Graphite Fiber Composites*. Van Nostrand Reinhold.

Shalin, R.E. (1995). *Polymer Matrix Composites* (1st ed). Chapman and Hall. https://books.google.com.cy/books?id=ubw_zEgOhr4C&lpg=PA2&pg=PA2#v=onepage&q&f=false

Shen, S., & Ishida, H. (1996). Development and characterization of high-performance polybenzoxazine composites., *Polymer Composites, 17,* 710-719. https://doi.org/ 10.1002/pc.10663

Rajak, D. K. (2019). Fiber-Reinforced Polymer Composites: Manufacturing. *Properties, and Applications., Polymers (Basel), 11(10)*, 1667. https://doi.org/ 10.3390/polym11101 667

Al-Haik, M., Borujeni, A.Y., & Tehrani, M. (2016). Ballistic damage of hybrid composite materials. *Advanced Fibrous Composite Materials for Ballistic Protection*, 121-143. https://doi.org/10.1016/B978-1-78242-461-1.00005-4

Rebouillat S. (2016). 2 - ARAMIDS: 'Disruptive', open and continuous innovation. *Advanced Fibrous Composite Materials for Ballistic Protection*, 11-70. https://doi.org/10.1016/B978-1-78242-461-1.00002-9

Okhawilai, M., & Rimdusit, S. (2017). Chapter 35 - Hard Armor Composites From Ballistic Fiber-Reinforced Polybenzoxazine Alloys A2. *Advanced and Emerging Polybenzoxazine Science and Technology, Elsevier*, Amsterdam, 699-723. https://doi.org/10.1016/B978-0-12-804170-3.00035-4

Che, D., Saxena, I., Han, P., & Guo P., (2014). Machining of carbon fiber reinforced plastics/polymers: A Literature Review. *Journal of Manufacturing Science and Engineering, 136(3).* https://doi.org/ 10.1115/1.4026526

Wang, X. M., & Zhang, L. C. (2003). An experimental investigation into the orthogonal cutting of unidirectional fibre reinforced plastics. *International Journal of Machine Tools and Manufacture, 43(10)*, 1015-1022. https://doi.org/10.1016/S0890-6955(03)00090-7

Dandekar, C. R., & Shin, Y. C. (2012). Modeling of Machining of Composite Materials: A Review. *International Journal of Machine Tools and Manufacture, 57*, 102–121. https://doi.org/10.1016/j.ijmachtools.2012.01.006

Ratna, D., Chongdar, T.K., & Chacraborty, B.C. (2004), Mechanical Characterization of New Glass Fiber Reinforced Epoxy Composite. *Polymer Composites, 25(2)*, 165-171. https://doi.org/10.1002 /pc.20013

Hallal, A., Younes, R., Fardoun, F., & Nehme, S. (2012). Improved analytical model to predict the effective elastic Dyna 176, 2012 123 properties of 2.5D interlock woven fabrics composite. *Composite Structures, 94(10)*, 3009-3028. https://doi.org/10.1016/j.compstruct.2012.03.019

Haim, A. (2017). 9 - Stability of composite stringer-stiffened panels. *Stability and vibrations of thin walled composite structures*, 461–507. https://doi.org/10.1016/B978-0-08-100410-4.00009-0

Colorado, H. A. Chaves Roldán, C., & Vélez, J. M., (2006). Internal Friction and Anaelstic Behavior in Solids. *Dyna (Medellin, Colombia), 73(148)*, 39-49. https://www.researchgate.net/publication/262666032

Wahab, Md.S., Rejab, M.N., & Saiman, M.P. (2014) Analysis of mechanical properties for 2D woven kenaf composite. Applied Mechanics and Materials, 660, 125-129. https://doi.org/10.4028/www.scientific.net/AMM.660.125

Cavallaro, P.V. (2016). Effects of Weave Styles and Crimp Gradients in Woven Kevlar/Epoxy Composites. *Experimental Mechanics, 56*, 617-635. https://doi.org/10.1007/s11340-015-0075-4

Ullah, H., Harland, A., & Silberschmidt V. (2014). Evolution and interaction of damage modes in fabric-reinforced composites under dynamic flexural loading. *Composites Science and Technology, 92*, 55–63. https://doi.org/10.1016/j.compscitech.2013.12.007

Cavallaro, P.V., & Sadegh, A.M., (2010). Crimp-Imbalanced Protective (Crimp) Fabrics. IMECE2010-40610, *Mechanics of Solids, Structures and Fluids, 9*, 331-349. https://doi.org/10.1115 /IMECE2010-40610

Gopinath, G., Zheng, J.Q., & Batra, R.C. (2012). Effect of matrix on ballistic performance of soft body armor. *Composite Structures, 94(9)*, 2690-2696. https://doi.org/10.1016/j.compstruct.2012.03.038

Okhawilai, M., Hiziroglu S., & Rimdusit S. (2018). Measurement of ballistic impact performance of fiber reinforced polybenzoxazine/polyurethane composites. *Measurement, 130*, 198-210. https:// doi.org/10.1016/j.measurement.2018.08.006

Chocron, S., Figueroa, E., King, N., Kirchdoerfer, T., Nicholls, A.E., Sagebiel, E., Weiss, C., & Freitas, C.J. (2010). Modeling and validation of full fabric targets under ballistic impact. *Composites Science and Technology, 70(13)*, 2012-2022. https:// doi.org/10.1016/j.compscitech.2010.07.025

Flores-Johnson, E.A., Shen, L., Guiamatsia, I., & Nguyen, G.D. (2014). Numerical investigation of the impact behavior of bioinspired nacre-like aluminum composite plates. *Composites Science and Technology,* 96, 13-22. https://doi.org/10.1016/ j.compscitech.2014.03.001

Ansari, M.M., & Chakrabarti, A. (2017). Influence of projectile nose shape and incidence angle on the ballistic perforation of laminated glass fiber composite plate, *Composites Science and Technology, 142*, 107-116. https://doi.org/ 10.1016/j.compscitech.2016.12.033

Sevkat, E., Liaw, B., Delale, F., & Raju, B.B. (2009). A combined experimental and numerical approach to study ballistic impact response of S2-glass fiber/toughened epoxy composite beams. *Composites Science and Technology, 69(7-8)*, 965-982. https://doi.org/10.1016/j.compscitech.2009.01.001

Naik, N., Sekher, YC., & Meduri, S., (2000). Damage in woven-fabric composites subjected to low-velocity impact. *Composites Science and Technology, 60(5)*, 731-744. https://doi.org/10.1016/S0266-3538(99) 00183-9

Ishida, H. (1996). Process for preparation of benzoxazine compounds in solventless systems. *United States Patents, 5,* 516. https://patentimages. storage.googleapis.com/f0/58/d7/88aa918889bd08/U S5543516.pdf

Inthakun, K. (2023). "Effects of Weave Structure on Mechanical Behavior of Carbon Fiber Fabric Reinforced Polybenzoxazine Composites. *CRMA Journal, 21*, 94-109. https://ph01.tci-thaijo.org/ index.php/crma-journal/issue/view/ 17392/4236

Tong, L., Mouritz, A.P., & Bannister, M.K. (2002). *3D Fiber Reinforced Polmer Composites* (1st ed.), Elsevier Science Ltd,. https://doi.org/10.1016/B978-0-08-043938-9.X5012-1

Ferris, T. (2024). Finite Element Analysis (FEA). Retrieved from https://www.ansys.com/simulation-topics/what-is-finite-element-analysis

Recht, R. F., & Ipson, T. W. (1963). Ballistic Perforation Dynamics. *In Journal of Applied Mechanics., 30(3),* 384-390. https://doi.org/10.1115/ 1.3636566

Colakoglu, M., Soykasap, O., & Özek, T. (2007). Experimental and numerical investigations on the ballistic performance of polymer matrix composites used in armor design, *Applied Composite Materials 14(1)*, 47-58. https://doi.org/10.1007/s10443-006-9030-y

Taraghi, I., Fereidoon, A., & Mohyeddin, A. (2014). The effect of MWCNTs on the mechanical properties of woven Kevlar/epoxy composites, *Steel and Composite Structures, 17(6)*, 825-834. https://doi.org/10.12989/scs.2014.17.6.825

Carrillo, J.G., Gamboa, R.A., Flores-Johnson, E.A., & Gonzalez-Chi, P.I. (2012). Ballistic performance of thermoplastic composite laminates made from aramid woven fabric and polypropylene matrix. *Polymer Testing. 31(4)*, 512-519. https://doi.org/10.1016/j. polymertesting.2012.02.010